Reac Kinet Mech Cat (2013) 108:1–16
DOI 10.1007/s11144-012-0510-9

Mechanism of the oxidative degradation of dibenzoazepine derivatives via manganese(III) complexes in acidic phosphate media

Joanna Wiśniewska · Paweł Rześnicki

Received: 6 July 2012 / Accepted: 13 October 2012 / Published online: 4 November 2012

Abstract The oxidative degradation of tricyclic antidepressants (TCA) was studied in the presence of a large excess of the oxidizing agents, manganese(III)-pyrophosphate ($P_2O_7^{4-}$), phosphate (PO_4^{3-}), in acidic media. The products were detected and identified using UV–Vis, ESI–MS and IR methods. The reaction between dibenz[b,f]azepines and manganese(III) ions proceeded via two consecutive reactions: first, acridine analogues were formed, and then a dealkylation process resulted in the formation of unsubstituted acridine. The kinetics of the first degradation step of the TCAs was investigated independently of the slower dealkylation step. The pseudo-first order rate constants (k_{obs}) were determined for the first degradation process. The reaction between 10,11-dihydro-5H-dibenz[b,f]azepines and the manganese(III) ion resulted in oxidative dehydrogenation, which proceeded via the formation of two intermediates: a free organic radical and a dimeric dication. Further oxidation of the second intermediate led to a positively charged radical dimer as a single final product. Simultaneously, two other substituent cleavage degradation processes occurred, which led to two dimeric derivatives. The kinetic traces were determined to be zeroth order.

Keywords Kinetics · Mechanism · Dibenzoazepine derivatives · Manganese(III) complexes

Electronic supplementary material The online version of this article (doi:10.1007/s11144-012-0510-9) contains supplementary material, which is available to authorized users.

J. Wiśniewska (✉) · P. Rześnicki
Department of Chemistry, Nicolaus Copernicus University, Gagarina 7, 87-100 Toruń, Poland
e-mail: wisnia@chem.uni.torun.pl

Introduction

Manganese complexes are well known in photosystem II as catalysts in the photolysis of water and in mitochondrial superoxide dismutase, which eliminates superoxide ions from eukaryotic cells [1–3]. A great deal of research investigated the design, synthesis, and evaluation of new catalysts used in the water splitting process and other biochemically important processes [4, 5]. Recently, a new series of manganese(III) complexes was reported as active scavengers of peroxynitrite ion, which is a potent proapoptotic species that plays a critical role in the aetiology of several forms of pain. Peroxynitrite ion is produced by the reaction between reactive oxygen species and nitric oxide [6, 7]. The manganese(III) complexes were reported to be effective oxidants for the degradation of many organic species [8, 9]. This paper focuses on the oxidative transformation of dibenzazepine derivatives. Extensive analyses of dibenzazepine compounds have shown a wide range of biological activities, including antidepressant, analgesic, antihistaminic, and antimuscarinic activities [10–19]. These nitrogen-containing heterocyclic compounds are used to manage neurogenic pain, attention-deficit hyperactivity disorder in children over the age of 6, depression, and a variety of other disorders (i.e., panic or phobic). Recently, dibenzazepine derivatives were shown to suppress cancer growth and induce apoptosis [20, 21]. A series of 11-phenyl-[b,e]-dibenzazepine compounds was determined to be inhibitors of tumor cell proliferation with IC50 values ranging from submicromolar to micromolar concentrations [22]. These compounds undergo a variety of metabolic processes in the human body, such as dealkylation and hydroxylation. Side effects (e.g., discoloration of the skin) may be caused by the oxidation of dibenzazepines to more highly reactive radical cations and their derivatives. Determining if dibenzazepine radical derivatives are present and how it can be produced would be of interest. How the process may occur in vivo in the presence of endogenous substances (e.g., oxidase and catalase, which include iron and manganese ions) is also of interest. Therefore, this study focused on the kinetics and mechanisms of the aqueous oxidative degradation by manganese(III) pyrophosphate, which was used as an example of a coordination metal ion that could mimic endogenous manganese-containing enzymes in living organisms and was a very effective metal-containing oxidant.

Experimental

Materials

Manganese(III) acetate ($Mn(CHCOO)_3 \cdot H_2O$), imipramine hydrochloride, desipramine hydrochloride, clomipramine hydrochloride, opipramol dihydrochloride, acetonitrile, formic acid and all other chemicals were analytical grade reagents from Sigma-Aldrich. Water that was purified in a Millipore Milli-Q system was used to prepare all of the solutions. Stock solutions of manganese(III) were prepared by dissolving manganese(III) acetate in 0.1 M $Na_4P_2O_7$ and 1.0 M H_3PO_4. Manganese(III) pyrophosphate is unstable at higher temperatures and undergoes a

disproportionation reaction [23]. Therefore, the stock solutions were freshly prepared before each series of kinetic measurements. Aqueous solutions of imipramine (Sigma-Aldrich) and other dibenzazepine derivatives were stored in a refrigerator at 5 °C.

Spectroscopic measurements

IR spectra were acquired using a Perkin-Elmer Spectrum 2000 Fourier Transform Infrared spectrometer using KBr discs (4,000–400 cm^{-1}). MS measurements were performed on a HPLC system 1100 (Agilent Technologies, Waldbronn, Germany) equipped with a quaternary pump and a UV–Vis detector, which was coupled with an Agilent 6410 Triple Quad LC/MS mass spectrometer equipped with an ESI ion source, a capillary voltage of 4.5 kV, a drying gas temperature of 300 °C, a flow of 9.0 l/min and a nebulizer pressure of 40 psi. Mass spectra were acquired in the full-scan positive mode with a mass-to-charge ratio (m/z) range from 100 to 850. Chromatographic separations were performed with a C18 column (Waters, 100 mm length × 2.1 mm i.d.) prior to the MS analysis. The composition of the mobile phase was on a gradient as follows: (A) water containing 0.2 % formic acid and (B) acetonitrile containing 0.2 % formic acid.

Kinetic measurements

For the imipramine, desipramine and clomipramine reactions, the stopped-flow measurements were performed on a Carl Zeiss Jena VSU2-G equipped with a home-made stopped-flow accessory. The reaction rate was recorded by monitoring the appearance of the product(s) visualized by an increase in absorbance of the characteristic electronic transition band(s). In the visible region of the spectrum, the characteristic electronic transition of the manganese(III)-pyrophosphate ions was observed, λ_{max}, nm (ε_{max}, $dm^3\ mol^{-1}\ cm^{-1}$): 513(85) [24]. The experimental conditions used for the oxidative degradation of imipramine, desipramine and clomipramine were as follows: $[TCA] = 5 \times 10^{-5}$ M, $[Mn^{III}] = (0.5–4.5) \times 10^{-3}$ M, $[Na_4P_2O_7]_T = 0.1$ M, $[H_3PO_4]_T = 1.0$ M, $[H^+] = 0.04$ M, $I = 0.45$ M (H^+, $H_2PO_4^-$, Na^+, $H_3P_2O_7^-$, $H_2P_2O_7^{2-}$), $T = 298$ K, $\lambda = 455$, 620, 698 nm. In another series of experiments, the dependence of the reaction rate on the H^+ concentration was determined: $[TCA] = 5 \times 10^{-5}$ M, $[Mn^{III}] = 2.5 \times 10^{-3}$ M, $[Na_4P_2O_7]_T = 0.1$ M, $[H_3PO_4] = 0.15–1.0$ M, $[H^+] = 0.0001–0.04$ M, $I = 0.40–0.45$ M (H^+, $H_2PO_4^-$, Na^+, $H_3P_2O_7^-$, $H_2P_2O_7^{2-}$), $T = 298$ K, $\lambda = 620$ nm. The time scales were 75–250 s, 75–250 s and 150–500 s (95 %) for imipramine, desipramine and clomipramine, in order. The zeroth order rate constants $k_1^{(0)}$ were determined by a linear least squares fit to the zeroth order dependence of absorbance (A) versus time (t) according to the following equation: $A = \text{constant} + l \cdot \Delta\varepsilon \cdot k_1^{(0)} \cdot t$, where $\Delta\varepsilon$ is the difference in the molar absorption coefficients for the reactant and product, and l is the optical path length. The relative standard errors for the zeroth order rate constants for a single kinetic trace and mean values were ca 0.5–1 % each.

For the reactions of opipramol, the kinetic measurements were acquired on a Shimadzu UV-1601 PC spectrophotometer equipped with a six-position cell-holder. Kinetic data were acquired and processed using UVPC personal spectroscopy software. The solutions were maintained at the desired temperature (±0.1 °C) with an external Julabo F25 ultrathermostat for all measurements. The reaction was initiated by adding 0.025 cm^3 of an aqueous 0.004 M opipramol solution to a quartz cuvette, which contained 1.975 cm^3 of a solution of manganese(III) pyrophosphate ($P_2O_7^{4-}$), phosphate (PO_4^{3-}) at an appropriate concentration. The other experimental conditions were as follows: $[Mn^{III}] = (0.5–4.5) \times 10^{-3}$ M, $[Na_4P_2O_7]_T =$ 0.1 M, $[H_3PO_4]_T = 1.0$ M, $[H^+] = 0.04$ M, $I = 0.45$ M (H^+, $H_2PO_4^-$, Na^+, $H_3P_2O_7^-$, $H_2P_2O_7^{2-}$), $T = 298–308$ K, $\lambda = 350$ nm. The reaction rate was also analyzed at a variety of H_3PO_4 concentrations: $[TCA] = 5 \times 10^{-5}$ M, $[Mn^{III}] =$ 0.5×10^{-3} M, $[Na_4P_2O_7]_T = 0.1$ M, $[H_3PO_4]_T = 0.15–1.0$ M, $[H^+] = 0.0001–0.04$ M, $I = 0.40–0.45$ M (H^+, $H_2PO_4^-$, Na^+, $H_3P_2O_7^-$, $H_2P_2O_7^{2-}$), $T = 298$ K, $\lambda = 350$ nm. The pseudo-first order rate constants were calculated using a non-linear fitting procedure to the first order absorbance dependence versus time. At least three kinetic runs were recorded for every combination of reagent concentrations, and the rate constants are reported as the average values. The relative standard errors of the pseudo-first order rate constants for a single kinetic trace were ca 0.5–1 %, while the relative standard errors of the mean values were usually ca 1–2 %.

Results and discussion

The analyses of the products produced from the oxidative degradation of the tricyclic antidepressants were performed using high performance liquid chromatography, IR and mass spectroscopy. The radical and intermediate products were detected using EPR, ^1H NMR and ^{13}C NMR and these results were discussed in detail in our earlier study [25, 26]. There are two classes of dibenzazepine derivatives (dibenz[b,f]azepines and 10,11-dihydro-5H-dibenz[b,f]azepines), which react according to different mechanisms.

Spectroscopic and kinetic measurements of the reactions of dibenz[b,f]azepine derivatives

For the opipramol (dibenz[b,f]azepine derivative) reaction, two main fractions were observed in the chromatogram. The fractions were characteristic of reactant 1 (7.6 min) and product 2 (Scheme 1), which had a retention time of 5.0 min and was in relatively high abundance. The presence of the following characteristic fragmentation peaks for the following products were detected in the MS spectra: product 2: 350 ($M^{+\cdot}$), 171 (M–$C_{13}H_9N$), 143 (M–$C_{15}H_{13}N$); product 3: 366 (MH^+, low relative abundance); product 4: 180 (MH^+, low relative abundance); and product 5: 196 (MH^+, low relative abundance) m/z. The molecular ions and fragmentation peaks for reactant 1 were detected as follows: 364 (MH^+), 234 (M–$C_6H_{13}N_2O$), 171 (M–$C_{14}H_{10}N$), and 143 (M–$C_{16}H_{14}N$) m/z. As indicated above, the main product of the opipramol degradation was a substituted acridine

(product 2, Scheme 1), which was different from the C-nitrosation reaction of opipramol [27]. Acridine belongs to a group of nitrogen-containing heterocyclic PAH molecules, which have recently been suggested as possible causes for the spectra observed for interstellar medium, including the unidentified IR emission bands and diffuse interstellar bands [28, 29]. The byproduct of the oxidative degradation of the heterocyclic C10 carbon atom in dibenz[b,f]azepine derivative was methanol, identified by ^{1}H NMR spectroscopy in our earlier study [26].

In the IR spectrum of the product after the degradation reaction, a broad absorption band was observed at 3,400 cm^{-1}, which was attributed to $\nu(O-H)$, and a sharp absorption band at 1,063 cm^{-1}, which was ascribed to the $\nu(C-O)$ vibration in primary aliphatic alcohols, (Fig. 1, Table 1). The bands observed at 1,614 cm^{-1} were mainly attributed to $\nu(C=C)$ stretching modes, the bands in the range of 900–700 cm^{-1} were attributed to out-of-plane $\delta(C-H)$ vibrations, and the band at 1,171 cm^{-1} was ascribed to the in-plane $\delta(C-H)$ mode of the aromatic ring. These vibrational frequencies were significantly different from the analogous frequencies in the IR spectrum of the reactant, which indicates that more structural changes occurred in the tricyclic heterocycle than in the aliphatic substituent after the oxidative degradation occurred. Both the reactant and product showed distinct C–H, C–C and C–N vibrations in the region of 1,457–1,304 cm^{-1}, which corresponded to vibrations in the aliphatic substituent. The vibrational frequencies observed at 1,266 cm^{-1}, which were assigned to the in-plane $\delta(C-H)$ vibration of the C9 carbon in the central acridine ring, were observed in all acridine derivatives [30]. These data indicate that the product that was observed in the IR spectrum was a substituted acridine, which was assigned as 10-[3-[4-(2-hydroksyethyl)-1-piperazinyl]propyl]-acridine (product 2, Scheme 1).

The oxidative degradation of dibenz[b,f]azepine derivatives (Scheme 1) proceeds in many steps: the first step is the formation of 10-[3-[4-(2-hydroxyethyl)-1-piperazinyl]propyl]-acridine. The second step, the conversion of 10-[3-[4-(2-hydroxyethyl)-1-piperazinyl]propyl]-acridine into unsubstituted derivative as the

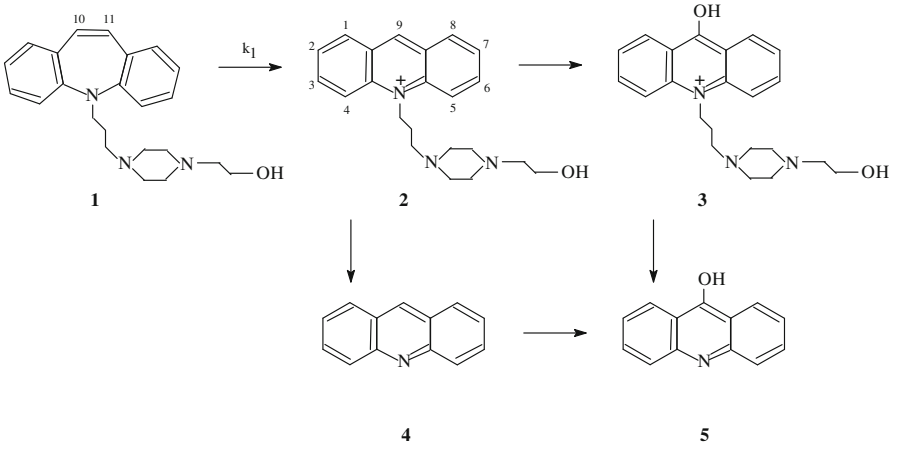

Scheme 1 Products in the oxidative degradation reaction of dibenz[b,f]azepine derivative

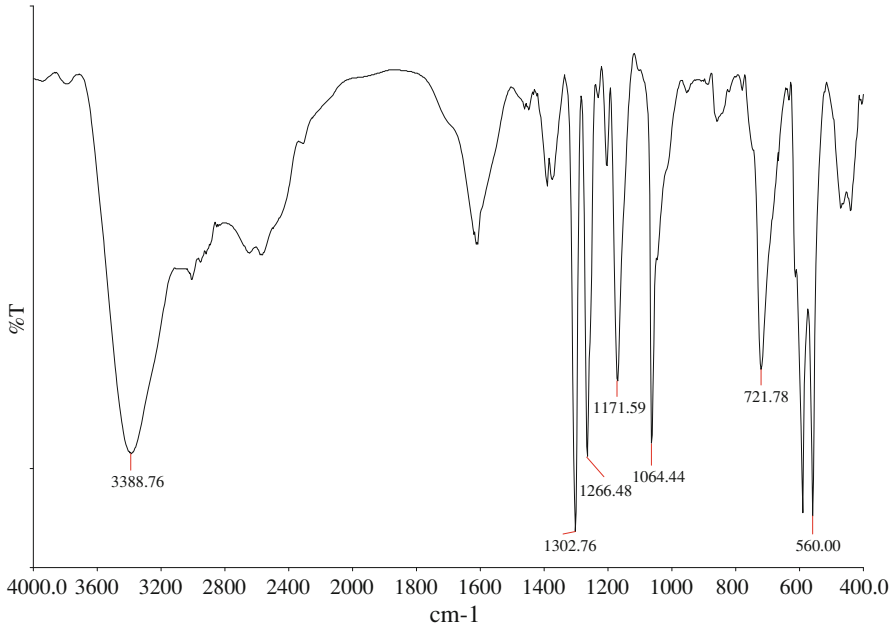

Fig. 1 FT-IR spectrum of 10-[3-[4-(2-hydroxyethyl)-1-piperazinyl]propyl]-acridine (product 2, Scheme 1), a product of the reaction between opipramol and the manganese(III) ion 4,000–400 cm^{-1} in a KBr disc

Table 1 Experimental vibrational frequencies of opipramol and 10-[3-[4-(2-hydroxyethyl)-1-piperazinyl]propyl]-acridine (product 2, Scheme 1) over the range of 4,000–400 cm^{-1} using a KBr disc

Frequencies (cm^{-1})	Frequencies (cm^{-1})	Vibration assignment
Opipramol	Acridine derivative	
3,333	3,389	ν(O–H) in the primary aliphatic alcohols
3,048	3,002	ν(C–H) in the aromatic ring
2,923	Two weak bands	ν(C−H) in the aliphatic chain
2,829		ν(C–H) in the aliphatic chain
2,600−2,300	2,600–2,300	Overtones in the aromatic ring
1,592	1,614	ν(C=C) in the aromatic ring
1,574	1,547	ν(C=N) in the aromatic ring
1,495		νC=C) in the aromatic ring
1,439	1,457	δ(C–H) of the $–CH_2–$in the aliphatic chain
1,393	1,387	ν(C–C) in the aliphatic chain
1,325	1,303	ν(C–N) in the aliphatic chain
	1,266	δ(C–H) in-plane for the heterocyclic C9 atom
1,071	1,172	δ(C–H) in-plane in the aromatic ring
1,059	1,064	ν(C–O) in the primary aliphatic alcohols
790	859	δ(C–H) out-of-plane in the aromatic ring
765	722	δ(C–H) out-of-plane in the aromatic ring

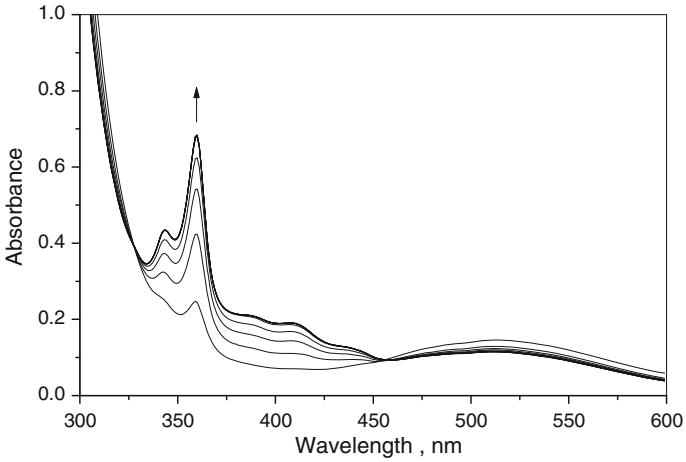

Fig. 2 Spectral changes observed during the oxidative degradation of opipramol using the manganese(III) ion. Experimental conditions: $[TCA] = 5 \times 10^{-5}$ M, $[Mn^{III}] = 1.5 \times 10^{-3}$ M, $[Na_4P_2O_7]_T = 0.1$ M, $[H_3PO_4]_T = 1.0$ M, pH 1.4 (phosphate buffer), $I = 0.45$ M (H^+, $H_2PO_4^-$, Na^+, $H_3P_2O_7^-$, $H_2P_2O_7^{2-}$), $T = 298$ K, $t = 0$–720 s, $\Delta t = 120$ s

alkyl substituent is lost and the further steps lead to the products with a low yield. The reaction progress was monitored using UV–Vis spectrophotometry. As shown in Fig. 2, the oxidative degradation resulted in an increase in the absorbance of the electronic transition of the n-π^* band ($\lambda_{max} = 360$ nm), which was assigned to product 2 (Scheme 1). As the reaction progressed further, the decrease in the absorbance of the n-π^* band (not shown in Fig. 2) is attributed to the processes in which product 2 undergoes to products 3 and 4. The second, very slow process and further steps were not investigated.

Therefore, the following set of reactions is proposed to have occurred with the manganese(III) ion:

$$TCA + Mn(III) \rightarrow TCA^{\cdot+} + Mn(II) \quad (1)$$

$$TCA^{\cdot+} + Mn(III) \rightarrow \text{product 2} + CH_3OH + Mn(II)\,(\text{fast}) \quad (2)$$

The rate of the formation of the acridine derivative 2 was analyzed using first order kinetics. The pseudo-first order rate constants (k_{obs}) are shown in Table 2. The reaction was assumed to be irreversible, and the observed rate constant was linearly dependent on $[Mn^{III}]$ (Fig. 3). The linear regression data are shown in Table 3. The intercept and the slope were assigned as the first (k_{-1}) and second-order rate constant (k_1) for the reaction between opipramol and manganese(III), respectively. The k_{-1} value was close to zero and was omitted in the second order rate law for the oxidative degradation of dibenz[b,f]azepines:

$$d[P]/dt = k_1 [Mn^{III}][TCA] \quad (3)$$

The rate was slightly dependent on $[H^+]$ in the 0.005–0.045 M range. The rate decreased as the $[H^+]$ decreased, while no reaction was observed at $[H^+] < 0.005$.

Table 2 Observed pseudo-first order (k_{obs}) and observed zeroth order rate constants ($k_1^{(0)}$) for the reaction between dibenz[b,f]azepine and 10,11-dihydro-5H-dibenz[b,f]azepine derivatives and the manganese(III) ion. Experimental conditions: [TCA] = 5×10^{-5} M, $[Na_4P_2O_7]_T = 0.1$ M, $[H_3PO_4]_T = 0.3$–1.0 M, pH 2.2–1.4 (phosphate buffer), $I = 0.40$–0.45 M (H^+, $H_2PO_4^-$, Na^+, $H_3P_2O_7^-$, $H_2P_2O_7^{2-}$), $T = 298$ K

λ (nm)	pH	$[Mn^{III}]$ (M)	$10^3\ k_{obs}$ (s^{-1}) Opipramol	$10^7\ k_1^{(0)}$ (Ms^{-1}) Imipramine	$10^7\ k_1^{(0)}$ (Ms^{-1}) Desipramine	$10^7\ k_1^{(0)}$ (Ms^{-1}) Clomipramine
544	1.4	0.0,005	0.454 ± 0.02[a]	2.82 ± 0.05	3.10 ± 0.01	1.25 ± 0.10
	1.4	0.0015	1.23 ± 0.04[a]	5.52 ± 0.11	5.98 ± 0.05	2.72 ± 0.05
	1.4	0.0025	2.13 ± 0.06[a]	7.99 ± 0.17	8.97 ± 0.17	3.87 ± 0.03
	1.4	0.0035	3.13 ± 0.03[a]	11.0 ± 0.06	11.3 ± 0.05	5.28 ± 0.10
	1.4	0.0045	4.14 ± 0.05[a]	13.8 ± 0.34	14.4 ± 0.22	6.58 ± 0.05
620	1.4	0.0005	1.09 ± 0.03[b]	2.25 ± 0.03	3.10 ± 0.12	1.68 ± 0.06
	1.4	0.0015	3.23 ± 0.02[b]	4.24 ± 0.06	5.52 ± 0.09	3.78 ± 0.02
	1.4	0.0025	5.83 ± 0.14[b]	6.27 ± 0.06	7.93 ± 0.15	5.43 ± 0.06
	1.4	0.0035	8.53 ± 0.06[b]	7.86 ± 0.06	9.81 ± 0.15	7.29 ± 0.06
	1.4	0.0045	11.1 ± 0.18[b]	9.91 ± 0.06	13.0 ± 0.25	9.17 ± 0.06
698	1.4	0.0005	1.83 ± 0.03[c]	1.58 ± 0.08	2.66 ± 0.02	1.72 ± 0.04
	1.4	0.0015	4.89 ± 0.06[c]	3.10 ± 0.04	4.33 ± 0.02	4.09 ± 0.08
	1.4	0.0025	8.23 ± 0.20[c]	4.38 ± 0.04	6.31 ± 0.09	5.81 ± 0.04
	1.4	0.0035	11.7 ± 0.80[c]	5.91 ± 0.04	8.18 ± 0.09	7.30 ± 0.02
	1.4	0.0045	15.7 ± 0.20[c]	7.14 ± 0.01	10.4 ± 0.14	9.30 ± 0.02
620	2.22	0.0025	0.43 ± 0.07[b,d]	1.97 ± 0.03		
	1.92	0.0025	0.60 ± 0.01[b,d]	3.46 ± 0.03		
	1.75	0.0025	0.72 ± 0.01[b,d]	4.42 ± 0.06		
	1.63	0.0025	0.78 ± 0.01[b,d]	5.17 ± 0.03		
	1.54	0.0025	0.97 ± 0.04[b,d]	5.55 ± 0.06		
	1.48	0.0025	1.04 ± 0.06[b,d]	5.99 ± 0.06		
	1.44	0.0025	1.16 ± 0.01[b,d]	6.55 ± 0.06		
	1.43	0.0025	1.18 ± 0.05[b,d]	6.80 ± 0.06		

[a] 288 K, 350 nm

[b] 298 K, 350 nm

[c] 308 K, 350 nm

[d] $[Mn^{III}] = 0.0005$ M

As was shown in an earlier study, at a pH > 2, manganese(III) undergoes a further coordination reaction with pyrophosphates [31] or the coordinated ligand in manganese(III) is deprotonated [32]. These conclusions were supported by an expected blue shift of the electronic transition band from 513 to 479 nm (pH 5.5), which was caused by the coordination reaction or deprotonation of coordinated pyrophosphate. The hydrolysis of manganese(III) should be accompanied by a bathochromic shift, which is not observable in the visible range. Increasing the concentration of the manganese(III) complexes with two and three coordinated pyrophosphates or deprotonation of coordinated ligand in the manganese(III) ion results in a decrease in the redox potential. This will reduce the rate of the oxidation

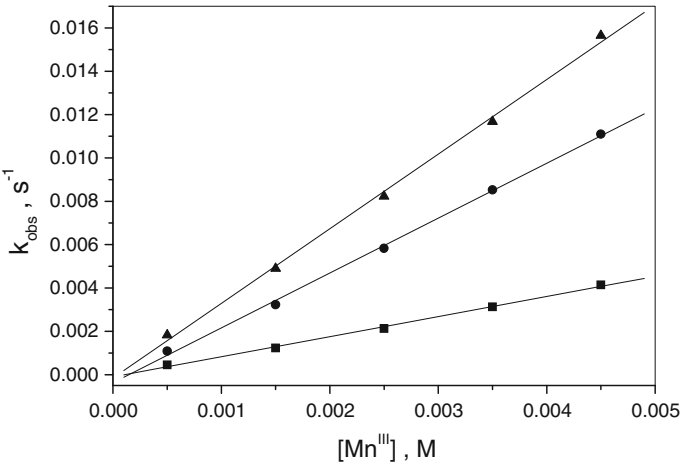

Fig. 3 Plots of k_{obs} versus [Mn^{III}] for the electron-transfer reaction between opipramol and the manganese(III) ion at various temperatures. Experimental conditions: [TCA] = 5×10^{-5} M, $[Na_4P_2O_7]_T = 0.1$ M, $[H_3PO_4]_T = 1.0$ M, pH 1.4 (phosphate buffer), $I = 0.45$ M (H^+, $H_2PO_4^-$, Na^+, $H_3P_2O_7^-$, $H_2P_2O_7^{2-}$), $T = 288$ (*filled square*), 298 (*filled circle*), 308 (*filled triangle*) K

Table 3 Linear regression data for the plots of k_{obs} versus [Mn^{III}] (Fig. 3) for the reaction between opipramol and the manganese(III) ion. Experimental conditions: [TCA] = 5×10^{-5} M, [Mn^{III}] = (0.5–4.5) $\times 10^{-3}$ M, $[Na_4P_2O_7]_T = 0.1$ M, $[H_3PO_4]_T = 1.0$ M, pH 1.4 (phosphate buffer), $I = 0.45$ M (H^+, $H_2PO_4^-$, Na^+, $H_3P_2O_7^-$, $H_2P_2O_7^{2-}$)

T (K)	k_1 ($M^{-1}s^{-1}$) Slope	$10^4\ k_{-1}$ (s^{-1}) Intercept
288	0.93 ± 0.03	−1.0 ± 0.8
298	2.53 ± 0.06	−3.7 ± 1.7
308	3.44 ± 0.09	−1.5 ± 2.7
$\Delta H^{\neq}$ (kJ mol^{-1})	36 ± 14	
$\Delta S^{\neq}$ (J $K^{-1}mol^{-1}$)	−117 ± 45	

reaction, which proceeds with an outer-sphere mechanism. Pyrophosphate exists in a few protolytic forms ($pK_{a1} = 0.81$, $pK_{a1} = 2.1$, $pK_{a1} = 6.44$, $pK_{a1} = 8.91$). Appropriate equilibrium constants (K_i) are presented in Table S1, ESI [33–35]. The $H_3P_2O_7^-$ ion dominates in the solution at pH 1–2. Coordination of pyrophosphate to manganese(III) enables deprotonation of the $H_3P_2O_7^-$ ion and a certain percentage (ϕ_i), of aqua and pyrophosphate-manganese(III) complexes results at low concentration of $[Na_4P_2O_7]_T < 0.01$ M, but at $[Na_4P_2O_7]_T = 0.1$ M, the manganese(III) complex with three coordinated pyrophosphates, $[Mn(H_2P_2O_7)_3]^{3-}$, dominates in the solution (99 %). The influence of the H^+ ion on the reaction rate results from deprotonation of a free ligand, $H_3P_2O_7^-$ and changes in the percentage of various coordination metal ions or results from deprotonation coordinated ligand in $[Mn(H_2P_2O_7)_3]^{3-}$.

This last assumption leads to the conclusion that manganese(III) exists in two equilibrium forms, $[Mn(H_2P_2O_7)_3]^{3-}$ and $[Mn(HP_2O_7)(H_2P_2O_7)_2]^{4-}$ at pH 1–2, $[Na_4P_2O_7]_T = 0.1$ M.

$$\left[Mn(H_2P_2O_7)_3\right]^{3-} \rightarrow \left[Mn(HP_2O_7)(H_2P_2O_7)_2\right]^{4-} + H^+ \quad (4)$$

$$K_a = [Mn(HL)][H^+]/[Mn(H_2L)] \quad (5)$$

$$[Mn]_T = [Mn(H_2L)] + [Mn(HL)] \quad (6)$$

where $[MnH_2L]$ and $[MnHL]$ refer to concentration of $[Mn(H_2P_2O_7)_3]^{3-}$ and $[Mn(HP_2O_7)(H_2P_2O_7)_2]^{4-}$, respectively. The percentage of the sum ($[Mn(H_2L)] + [Mn(HL)]$) did not change significantly at pH 1–2 and is equal to 99 %, therefore, we can assume that $[Mn(H_2L)]_T = [Mn]_T$. The required species concentrations can be obtained from the mass balance Eqs. 4 and 6 for manganese(III), combined with expression 5 for the equilibrium constants.

$$[MnH_2L] = [Mn]_T[H^+]/(K_a + [H^+]) \quad (7)$$

$$[MnHL] = K_a[Mn]_T/(K_a + [H^+]) \quad (8)$$

The overall rate of product formation is the sum of the individual rate terms, Eq. 9.

$$d[P]/dt = (k_{1a}[Mn(H_2L)] + k_{1b}[Mn(HL)])[TCA] \quad (9)$$

Upon inserting the expressions for the concentrations of the reacting species into Eq. 9 and rearrangement, one obtains the full kinetic equation given in Eq. 10.

$$d[P]/dt = (k_{1a}[H^+] + k_{1b})[Mn]_T[TCA]/(K_a + [H^+]) \quad (10)$$

The observed first (k_{obs}) and second (k) order rate constants can be written as in Eq. 11.

$$k = k_{obs}/[Mn]_T = (k_{1a}[H^+] + k_{1b})/(K_a + [H^+]) \quad (11)$$

The parameters k_{1a}, k_{1b}, and K_a are listed in Table 4. A similar dependence was also observed in the reaction of the second class of dibenzazepine derivatives (10,11-dihydro-5H-dibenz[b,f]azepines). The fitting results for the parameters of Eq. 11 for opipramol at $\lambda = 350$ nm lead to the following rate constant values: $k_{1a} = 4.63 \pm 1.13$ $M^{-2}s^{-1}$, $k_{1b} = (4 \pm 6) \times 10^{-3}$ $M^{-1}s^{-1}$, $K_a = 0.04 \pm 0.02$ M, $pK_a = 1.4$. The value of $pK_a = 1.4$ for the coordinated $H_2P_2O_7^{2-}$ is significantly lower than the value of $pK_{a3} = 6.44$ for the free $H_2P_2O_7^{2-}$ ligand (Table S1, ESI) but is similar to $pK_a = 1.5$ in the reaction of imipramine (see further discussion). These results suggest that manganese(III) exists as $[Mn(H_2P_2O_7)_3]^{3-}$ and $[Mn(HP_2O_7)(H_2P_2O_7)_2]^{4-}$ in the solution at pH 1–2.

Spectroscopic and kinetic measurements of the 10,11-dihydro-5H-dibenz[b,f]azepine derivatives reaction

The second class of dibenzazepine derivatives (10,11-dihydro-5H-dibenz[b,f]azepines) reacts according to different mechanism and leads to different products. In

Table 4 Non-linear regression data for the plots of $k_{obs}/[Mn]_T$ or $k_1^{(0)}/[Mn]_T$ versus $[H^+]$ (Fig. 6) for the reaction between dibenz[b,f]azepine and 10,11-dihydro-5H-dibenz[b,f]azepine derivatives and the manganese(III) ion. Experimental conditions: $[TCA] = 5 \times 10^{-5}$ M, $[Mn^{III}] = 0.5 \times 10^{-3}$ M, $[Na_4P_2O_7]_T = 0.1$ M, $[H_3PO_4]_T = 0.15$–1.0 M, pH 4.0–1.4 (phosphate buffer), $I = 0.40$–0.45 M (H^+, $H_2PO_4^-$, Na^+, $H_3P_2O_7^-$, $H_2P_2O_7^{2-}$)

Parameter	Opipramol	Imipramine[a]
k_{1a} ($M^{-2}s^{-1}$)	4.63 ± 1.13	$(4.8 \pm 0.4) \times 10^{-4}$
k_{1b} ($M^{-1}s^{-1}$)	$(4 \pm 6) \times 10^{-3}$	$(0.4 \pm 2) \times 10^{-7}$
K_a (M)	0.04 ± 0.02	0.031 ± 0.006

[a] k_{1a} ($M^{-1}s^{-1}$), k_{1b} (s^{-1}), $[Mn^{III}] = 2.5 \times 10^{-3}$ M

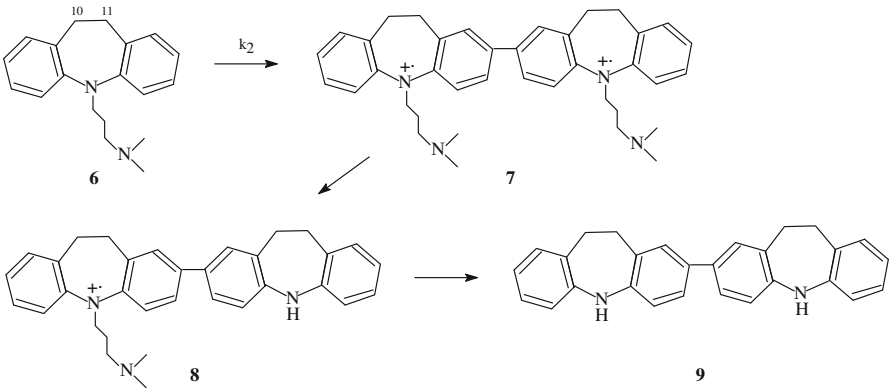

Scheme 2 Products in the oxidative degradation reaction of 10,11-dihydro-5H-dibenz[b,f]azepine derivative

the chromatogram acquired after the imipramine reaction, a fraction was observed that was characteristic for the reactant, which had a retention time of 9.8 min. In addition, a few other fractions were observed including products 7, 8, and 9 (Scheme 2), which had retention times of 9.2, 11.5, and 15.5 min. Fragmentation peaks of the products can be observed in the electrospray ionization MS spectra: product 7: 557 (M–H, high abundance), 472 (M–$C_5H_{12}N$), 279 (M–$C_{19}H_{22}N_2$ monomer) *m/z*, product 8: 474 (MH^+, high abundance), 388 (M–$C_5H_{12}N$), 86 (M–$C_{28}H_{24}N_2$) m/z; product 9: 388 ($M^{+\cdot}$, high abundance) m/z; the methyl derivative of 8: 488 (MH^+, low relative abundance) m/z; and the hydroxy derivative of 6: 297 (MH^+, low relative abundance), 279 (M–OH), 86 (M–$C_{14}H_{13}NO$) m/z. The molecular ions and fragmentation peaks for reactant 6 were detected as follows: 281 (MH^+), 236 (M–C_2H_6N), 208 (M–$C_4H_{10}N$), 86 (M–$C_{14}H_{12}N$), and 58 (M–$C_{16}H_{16}N$) m/z. The products that were detected were the same as the products detected in the reaction of 10,11-dihydro-5H-dibenz[b,f]azepines with peroxodisulfate in acidic media [26]. The spectrometric MS study indicated that in the case of 10,11-dihydro-5H-dibenz[b,f]azepines, oxidative degradation resulted in the formation of a few products (*i.e.*, the dimeric product 7, the dimeric product 8 with one substituent cleaved, and the dimeric product 9 with both substituents cleaved, see Scheme 2).

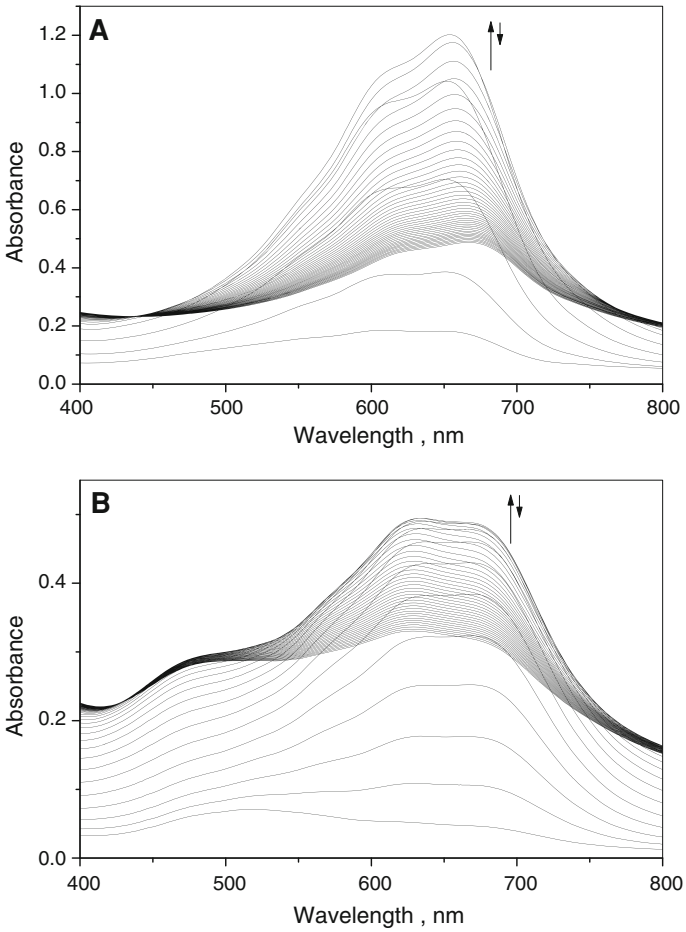

Fig. 4 Spectral changes observed during the oxidative degradation of 10,11-dihydro-5H-dibenz[b,f]-azepine derivatives using the manganese(III) ion. Experimental conditions: [TCA] = 5×10^{-5} M, $[Mn^{III}] = 5 \times 10^{-4}$ M, $[Na_4P_2O_7]_T = 0.1$ M, $[H_3PO_4]_T = 1.0$ M, pH 1.4 (phosphate buffer), $I =$ 0.45 M (H^+, $H_2PO_4^-$, Na^+, $H_3P_2O_7^-$, $H_2P_2O_7^{2-}$), $T = 298$ K. **A** imipramine, $t = 0$–1,350 s, **B** clomipramine, $t = 0$–630 s

The UV–Vis spectra provided evidence for the simultaneous formation of the intensively coloured dimer(s) (Fig. 4). Dimer 7 absorbs intensively in the visible region (Scheme 2) at 609 nm (λ_{lit}, nm (ε_{lit}, M^{-1} cm^{-1}): 625(29,300) [36]. The next product 8 is characterized by the electron transition band at 648 nm (λ_{lit}, nm (ε_{lit}, M^{-1} cm^{-1}): 670(33,000) [36]. An increase of absorbance over time, which corresponds to an increase in the concentration of the resultant dimer(s), was not characterized by the induction time as in the case of the reaction of TCA derivatives with $S_2O_8^{2-}$ [26]. The kinetic traces were linear (Fig. 5). A deviation was only observed from linearity for the lowest concentration of the manganese(III) ion. The characteristic sigmoidal shape indicated that the consecutive multiple-reaction scheme occurred for the 10,11-dihydro-5H-dibenz[b,f]azepine derivatives. After

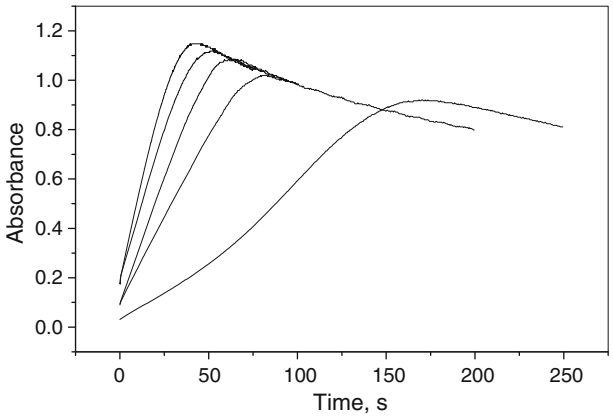

Fig. 5 Kinetic traces observed during the oxidative degradation of imipramine using the manganese(III) ion. Experimental conditions: $[TCA] = 5 \times 10^{-5}$ M, $[Mn^{III}] = 0.0005$–0.0045 M, $[Na_4P_2O_7]_T = 0.1$ M, $[H_3PO_4]_T = 1.0$ M, pH 1.4 (phosphate buffer), $I = 0.45$ M (H^+, $H_2PO_4^-$, Na^+, $H_3P_2O_7^-$, $H_2P_2O_7^{2-}$), $T = 298$ K

reaching maximum absorbance, as a result of the accumulation of product(s), a very slow decrease in absorbance was observed as a result of further degradation processes.

Therefore, the following set of reactions is proposed to have occurred with the manganese(III) ion:

$$TCA + Mn(III) \rightarrow TCA^{\cdot+} + Mn(II) \quad (12)$$

$$TCA^{\cdot+} + TCA^{\cdot+} \rightarrow (TCA)_2 + 2H^+ \quad (13)$$

$$(TCA)_2 + Mn(III) \rightarrow (TCA)_2^{\cdot+} + Mn(II) \quad (14)$$

$$(TCA)_2^{\cdot+} + Mn(III) \rightarrow (TCA^+)_2 + Mn(II) \quad (15)$$

$$(TCA^{\cdot+})_2 \rightarrow P \quad (16)$$

The oxidative degradation of 10,11-dihydro-5H-dibenz[b,f]azepine derivatives referred to the increase of absorbance was investigated using the zero-order kinetics (Fig. 5). The zeroth order rate constants ($k_1^{(0)}$) were calculated from the linear dependence of absorbance versus time (Experimental section), which enabled the regression data to be evaluated and are collected in Table 2. The reaction leads to different products, for that reason, the zeroth order rate constants were determined for any derivative at different wavelengths. The regression data (k_2 and k_{-2}) were calculated using a fitting procedure to the linear $k_1^{(0)}$ dependence versus $[Mn^{III}]$. The first order rate constants (k_2) refer to the slopes and are summarized in Table 5. The reaction was assumed to be irreversible due to the insignificant intercept values (k_{-2}) obtained. Thus, the first order rate law for the oxidative degradation of 10,11-dihydro-5H-dibenz[b,f]azepines can be expressed using the following equation:

$$d[P]/dt = k_2[Mn^{III}] \quad (17)$$

Table 5 Linear regression data for the plots of $k_1^{(0)}$ versus $[Mn^{III}]$ for the reaction between 10,11-dihydro-5H-dibenz[b,f]azepine derivatives and the manganese(III) ion. Experimental conditions: $[TCA] = 5 \times 10^{-5}$ M, $[Mn^{III}] = (0.5–4.5) \times 10^{-3}$ M, $[Na_4P_2O_7]_T = 0.1$ M, $[H_3PO_4]_T = 1.0$ M, pH 1.4 (phosphate buffer), $I = 0.45$ M (H^+, $H_2PO_4^-$, Na^+, $H_3P_2O_7^-$, $H_2P_2O_7^{2-}$)

λ (nm)	$10^4\ k_2$ (s^{-1}) Slope Imipramine	$10^7\ k_{-2}$ (Ms^{-1}) Intercept	$10^4\ k_2$ (s^{-1}) Slope Desipramine	$10^7\ k_{-2}$ (Ms^{-1}) Intercept	$10^4\ k_2$ (s^{-1}) Slope Clomipramine	$10^7\ k_{-2}$ (Ms^{-1}) Intercept
544	2.74 ± 0.05	1.4 ± 0.2	2.80 ± 0.06	1.8 ± 0.2	1.32 ± 0.04	0.6 ± 0.1
620	1.89 ± 0.04	1.4 ± 0.2	2.40 ± 0.10	1.9 ± 0.3	1.85 ± 0.06	0.8 ± 0.1
698	1.39 ± 0.03	0.9 ± 0.1	1.93 ± 0.05	1.5 ± 0.2	1.84 ± 0.14	1.0 ± 0.3

The first-order rate constants (k_2) represent the magnitude of the reactivity of this class of 10,11-dihydro-5H-dibenz[b,f]azepines and did not significantly differ among the derivatives (Table 5). Much more distinct differences in the values of the first order rate constants were determined for any derivative at different wavelengths. The electron-withdrawing Cl substituent in clomipramine was expected to induce a lower rate constant for the reaction between the manganese(III) ion and the drug; however, this phenomenon was not observed. The k_2 values for imipramine and clomipramine were determined to be 1.89×10^{-4} and 1.85×10^{-4} s^{-1}, respectively (at 620 nm, Table 5). In general, these results indicate that the reactivity of the TCA derivatives is similar in the reaction with the manganese(III) ion. The higher reactivity of the phenothiazine derivatives would be expected for simple electron transfer processes, because the presence of the sulfur atom decreases the reduction potential [37]. This phenomenon is not observed in the reaction with the manganese(III) ion, [24]. The reactivity of the 10,11-dihydro-5H-dibenz[b,f]azepine derivatives is similar to the dibenz[b,f]azepine derivatives. However, oxidative degradation leads to different products.

The rate was dependent on $[H^+]$ as in the reaction of opipramol (dibenz[b,f]azepine derivatives). Thus, the overall rate of the product formation is as follows:

$$d[P]/dt = (k_{1a}[H^+] + k_{1b})[Mn]_T/(K_a + [H^+]) \quad (18)$$

and leads to the same expression as Eq. 11. Fitting results for the parameters of Eq. 11 for imipramine at $\lambda = 620$ nm are presented in Fig. 6 and leads to the following values of rate constants: $k_{1a} = (4.8 \pm 0.4) \times 10^{-4}$ $M^{-1}s^{-1}$, $k_{1b} = (0.4 \pm 2) \times 10^{-7}$ s^{-1}, $K_a = 0.031 \pm 0.006$ M, $pK_a = 1.5$.

The kinetics of the degradation of the dimer(s) and their derivatives referred to the decrease of absorbance (Fig. 5, Eq. 16) was first order. However, as shown in Fig. 6, the rate of the degradation process was independent of the manganese(III) concentration, which indicated that this process was not induced or caused by further oxidation. Furthermore, the rate constants for the degradation of imipramine and desipramine dimers were similar, $(2.90 \pm 0.006) \times 10^{-3}$ s^{-1} and $(2.92 \pm 0.005) \times 10^{-3}$ s^{-1}, $[TCA] = 5 \times 10^{-5}$ M, $[Mn^{III}] = 5 \times 10^{-4}$ M, $[Na_4P_2O_7]_T = 0.1$ M, $[H_3PO_4]_T = 1.0$ M, pH 1.4 (phosphate buffer), $I = 0.45$ M (H^+, $H_2PO_4^-$,

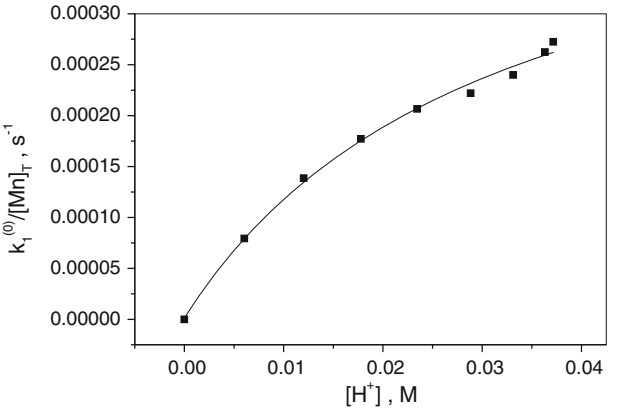

Fig. 6 Plot of $k_1^{(0)}/[Mn]_T$ versus $[H^+]$ for the electron-transfer reaction between imipramine and the manganese(III) ion. Experimental conditions: $[TCA] = 5 \times 10^{-5}$ M, $[Mn^{III}] = 2.5 \times 10^{-3}$ M, $[Na_4P_2O_7]_T =$ 0.1 M, $[H_3PO_4]_T = 0.15$–1.0 M, pH 4.0–1.4 (phosphate buffer), $I = 0.40$–0.45 M (H^+, $H_2PO_4^-$, Na^+, $H_3P_2O_7^-$, $H_2P_2O_7^{2-}$), $T = 298$ K

Na^+, $H_3P_2O_7^-$, $H_2P_2O_7^{2-}$), $T = 298$ K, $\lambda = 620$ nm. However, a slight deviation from first order kinetics was observed for clomipramine, $(1.27 \pm 0.002) \times 10^{-3}$ s^{-1}, which was primarily due to the generation of the intermediate product and further degradation to a final product, that partially precipitated. In Fig. 4B, the characteristic electronic transition band observed with a maximum that occurred at 525 nm probably can be attributed to the intermediate.

Acknowledgments The authors thank Mr. Grzegorz Spólnik (Department of Organic Chemistry, Polish Academy of Science, Warsaw) for help with the MS measurements and Mrs. Aleksandra Mosińska (Department of Chemistry, Nicolaus Copernicus University, Toruń) for help with the experimental work.

References

1. Ferreira KN, Iverson TM, Maghlaoui K, Barber J, Iwata S (2004) Science 303:1831–1838
2. Riggs-Gelasco PJ, Mei R, Penner-Hahn JE (1996) Adv Chem 246:219–248
3. Dau H, Haumann M (2008) Coord Chem Rev 252:273–295
4. Berggren G, Thapper A, Huang P, Eriksson L, Styring S, Anderlund MF (2011) Inorg Chem 50:3425–3430
5. Jin N, Lahaye DE, Groves JT (2010) Inorg Chem 49:11516–11524
6. Rausaria S, Kamadulski A, Rath NP, Bryant L, Chen Z, Salvemini D, Neumann WL (2011) J Am Chem Soc 133:4200–4203
7. Rausaria S, Ghaffari MME, Kamadulski A, Rodgers K, Bryant L, Chen Z, Doyle T, Shaw MJ, Salvemini D, Neumann WL (2011) J Med Chem 54:8658–8669
8. Wang G-W, Wang C-Z, Zou J-P (2011) J Org Chem 76:6088–6094

9. Cao J, Miao M, Chen W, Wu L, Huang X (2011) J Org Chem 76:9329–9337
10. Ashby J, Elliott BM (1984) In: Katritzky AR, Rees CW Meth-Cohn O (eds) Comprehensive heterocyclic chemistry, Pergamon Press: Oxford, Vol 1, pp 111–183
11. Pozharskii AF, Soldatenkov AT (1997) Katritzky AR In Heterocycles in Life and Society. John Wiley & Sons, New York
12. Liegeois JFF, Rogister FA, Bruhwyler J, Damas J, Nguyen TP, Inarejos MO, Chleide EMG, Mercier MGA, Delarge JE (1994) J Med Chem 37:519–525
13. Blache Y, Hichour M, Di Blasi G, Chezal J-M, Viols H, Chavignon O, Teulade J-C, Chapat J-P (1999) Heterocycles 51:1003–1014
14. Heinisch G, Huber E, Matuszczak B, Mereiter K (1999) Heterocycles 51:1035–1050
15. Link A, Kunick C (1998) J Med Chem 41:1299–1305
16. Grunewald GL, Galdwell TM, Li Q, Criscione KR (2001) J Med Chem 44:2849–2856
17. Kling A, Backfish G, Delzer J, Geneste H, Graef C, Holzenkamp U, Hornberger W, Lange UEW, Lauterbach A, Mack H, Seitz W, Subkowski T (2002) Bioorg Med Chem Lett 12:441–446
18. Andrés JI, Alonso JM, Fernández J, Iturrino L, Martínez P, Meert TF, Sipido VK (2002) Bioorg Med Chem Lett 12:3573–3577
19. Li R, Tränkle C, Mohr K, Holzgrabe U (2001) Arch Pharm 334:121–124
20. Sakurada K, McDonald FM, Shimada F (2008) Angew Chem Int Ed 47:5718–5738
21. Shih IM, Wang TL (2007) Cancer Res 67:1879–1882
22. Al-Qawasmeh RA, Lee Y, Cao MY, Gu X, Viau S, Lightfoot J, Wright JA, Young AH (2009) Bioorg Med Chem Lett 19:104–107
23. Klewicki JK, Morgan JJ (1998) Environ Sci Technol 32:2916–2922
24. Wiśniewska J, Rześnicki P, Topolski A (2011) Trans Met Chem 36:767–774
25. Wiśniewska J, Wrzeszcz G, Kurzawa M, van Eldik R (2012) Dalton Trans 41:1259–1267
26. Wiśniewska J, Wrzeszcz G, Koter S, Ligor T (2012) React Kinet Mech Cat 107:1–17
27. Faigle JW, Blattner H, Glatt H, Kriemler H-P, Mory H, Storni A, Winkler T, Oesch F (1987) Helv Chim Acta 70:1296–1301
28. Tielens AGGM (2008) Annu Rev Astron Astrophys 46:289–337
29. Alvaro Galué H, Pirali O, Oomens J (2010) Astron Astrophys 517:1–11
30. Lagutschenkov A, Dopfer O (2011) J Mol Spec 268:66–77
31. Watters JI, Kolthoff IM (1948) J Am Chem Soc 70:2455–2460
32. Bozor I, Simándi LI (2002) J Chem Soc Dalton Trans 3226–3233
33. Martell AE, Smith RM, Motekaitis RJ (2004) NIST critically selected stability constants of metal complexes database US department of commerce. National Institute of Standards and Technology, Gaithersburg
34. Ciavatta L, Palombari R (1983) Gazz Chim Ital 113:557–562
35. Gordienko VI, Sidorenko VI, Mikhailyuk YI (1970) Russ J Inorg Chem Ingl Transl 15:1241
36. Horria AM (1992) Anal Lett 25:63–71
37. García C, Oyola R, Piñero L, Hernández D, Arce R (2008) J Phys Chem B 112:168–178